Chemistry and Physics of Lipids 205 (2017) 1–10

Contents lists available at ScienceDirect

Chemistry and Physics of Lipids

journal homepage: www.elsevier.com/locate/chemphyslip

Effects of seaweed sterols fucosterol and desmosterol on lipid membranes

Ole G. Mouritsen[a,*], Luis A. Bagatolli[a,b], Lars Duelund[a], Olav Garvik[a], John H. Ipsen[a], Adam Cohen Simonsen[a]

[a] MEMPHYS – Center for Biomembrane Physics, University of Southern Denmark, Campusvej 55, DK-5230 Odense M, Denmark
[b] Yachay EP and Yachay Tech, Yachay City of Knowledge, Ecuador[1]

ARTICLE INFO

Article history:
Received 9 March 2017
Received in revised form 27 March 2017
Accepted 27 March 2017
Available online 30 March 2017

Keywords:
Higher sterols
Cholesterol
Fucosterol
Desmosterol
Ergosterol
Lipid bilayers
Phase behavior
Membrane mechanics
Lipid domains
Seaweed

ABSTRACT

Higher sterols are universally present in large amounts (20–30%) in the plasma membranes of all eukaryotes whereas they are universally absent in prokaryotes. It is remarkable that each kingdom of the eukaryotes has chosen, during the course of evolution, its preferred sterol: cholesterol in animals, ergosterol in fungi and yeast, phytosterols in higher plants, and e.g., fucosterol and desmosterol in algae. The question arises as to which specific properties do sterols impart to membranes and to which extent do these properties differ among the different sterols. Using a range of biophysical techniques, including calorimetry, fluorescence microscopy, vesicle-fluctuation analysis, and atomic force microscopy, we have found that fucosterol and desmosterol, found in red and brown macroalgae (seaweeds), similar to cholesterol support liquid-ordered membrane phases and induce coexistence between liquid-ordered and liquid-disordered domains in lipid bilayers. Fucosterol and desmosterol induce acyl-chain order in liquid membranes, but less effectively than cholesterol and ergosterol in the order: cholesterol > ergosterol > desmosterol > fucosterol, possibly reflecting the different molecular structure of the sterols at the hydrocarbon tail.

1. Introduction

Higher sterols are believed to serve as important modulators of the physical properties and lateral molecular organization of the fluid-bilayer component of cell plasma membranes. Due to their rigid and molecularly smooth and flat steroid ring structure, the sterols order the acyl chain of the phospholipids in liquid (fluid) lipid membranes leading to membrane thickening, decreased permeability, and a substantial mechanical stiffening of the bilayers (Mouritsen and Zuckermann, 2004). At the same time the sterols maintain the fluidity and fast lateral molecular diffusion in the membranes necessary for membrane function (Mouritsen and Bagatolli, 2016), e.g., by fluidizing lipid membranes in their solid (gel) states.

The differential effects of sterols on liquid and solid membrane phases, so pronouncedly reflected in their peculiar phase diagram involving coexistence between two different liquid phases, is believed to be an important signature of sterol effects in both model membranes (Bagatolli et al., 2010) as well as functional biological membranes (Simons and Sampaio, 2011). Most importantly, the higher sterols cholesterol (Vist and Davis, 1990; Ipsen et al., 1987; Davis et al., 2009, 2013; Alsop et al., 2016), ergosterol (Hsueh et al., 2005, 2007), and dehydroergosterol (Garvik et al., 2009) have been demonstrated in some binary, and in the case of cholesterol also in several ternary (Feigenson and Buboltz, 2001; Marsh, 2009; Heberle et al., 2010; Bezlyepkina et al., 2013) as well as quaternary (Konyakhina et al., 2013) lipid mixtures to promote a special membrane phase, the so-called liquid-ordered phase, that is a liquid phase with high molecular diffusion rates but with ordered lipid acyl chains (Ipsen et al., 1987; Mouritsen, 2010).

It has been surmised that only higher sterols can promote the liquid-ordered phase (Miao et al., 2002), whereas precursors in the sterol biosynthetic pathway, such as lanosterol, cannot (Bloom and Mouritsen, 1995; Aittoniemi et al., 2006). The liquid-ordered phase forms the biophysical basis for the so-called 'raft' hypothesis that assigns functional properties to nano-scale lipid domains in membranes (Simons and Sampaio, 2011; Sezgin et al., 2012). A wide range of model membranes and reconstituted membranes

* Corresponding author.
E-mail address: ogm@memphys.sdu.dk (O.G. Mouritsen).
URL: http://www.memphys.sdu.dk (O.G. Mouritsen)
[1] Present address.

http://dx.doi.org/10.1016/j.chemphyslip.2017.03.010
0009-3084/

Nomenclature

Abbreviations

AFM	atomic force microscopy
DOPC	1,2-dioleoyl-*sn*-glycero-3-phosphocholine
$DiIC_{18}$	1,1′-dioctadecyl-3,3,3′,3′-tetramethylindocarbocyanine perchlorate
DSC	differential scanning calorimetry
DPPC	1,2-dipalmitoyl-*sn*-glycero-3-phosphocholine
GP	generalized polarization
GUV	giant unilamellar vesicle
LAURDAN	6-lauroyl-2-(dimethylamino)-naphthalene
Naphthopyren	naphtho[2,1,8-qra]naphthacene
N-Rh-DPPE	Lissamine rhodamine B 1,2-dihexadecanoyl-sn-glycero-3-phosphoethanolamine
POPC	1-palmitoyl-2-oleoyl-*sn*-glycero-3-phosphocholine

Sterols

cholesterol	cholest-5-en-3β-ol
desmosterol	cholesta-5,24-dien-3β-ol
ergosterol	ergosta-5,7,22-trien-3β-ol
fucosterol	24-ethylcholesta-5,24(28)-dien-3β-ol

with and without proteins have been shown to display lateral domain structure (Bagatolli et al., 2010; Mouritsen, 2011; Almeida, 2014) although it still remains controversial whether rafts exists in functional cell membranes (Jacobson et al., 2007; Sevcsik and Schütz, 2015). A particular issue has been the sizes and timescales associated with putative rafts in both model systems and biological membranes, what type of local structures these lipid domains and rafts may have, and what their local structure and dynamics may be (Almeida et al., 2005; Armstrong et al., 2013; Rheinstädter and Mouritsen, 2013; Alsop et al., 2016).

Whereas there is a substantial literature on the effect of the animal sterol cholesterol on membrane structure, there are surprisingly few quantitative studies delineating the effect on membrane structure of sterols from higher plants (Hodzic et al., 2008; Shaghaghi et al., 2016; Beck et al., 2007; Grosjean et al., 2015), fungi (Hsueh et al., 2005, 2007), and marine algae (Dai et al., 1991; Simonsen et al., 2009). The question naturally arises whether algae sterols conform to the known universal behavior of animal and fungal sterols in terms of increased membrane ordering, reinforced mechanics, and stabilization of a liquid-ordered phase or domains with liquid-ordered chains. The answer to this question may be important not only for understanding algae physiology (Patterson, 1991; Ilias et al., 2006) but also for human nutrition and health as it appears that sterols, in particular algal sterols, have positive effects on human health, such as improved digestion, enhanced blood clearance, and lowering of free and bound cholesterol (Tapiero et al., 2002; Yi et al., 2016).

Here we pose this question in the case of the algae sterols fucosterol and desmosterol. Fucosterol is a principal sterol in brown macroalgae, e.g., *Macrocystis* and members of Laminariales family, whereas desmosterol is a dominating sterol in many red macroalgae, e.g., *Pyropia* and *Palmaria* (Patterson, 1991).

In the present paper we have performed a comparative biophysical study between cholesterol and the algae sterols desmosterol and fucosterol (see Fig. 1 for structural formulas). We have also performed some selected studies involving cholesterol and the fungal sterol ergosterol. In comparison with cholesterol, desmosterol and fucosterol have modifications at the hydrocarbon tail; desmosterol with a double bond at position 24–25 and fucosterol with a branched chain and a double bond at position 24. Ergosterol has the same hydrocarbon tail as cholesterol, but an additional double bond between positions 7 and 8 at the fused ring structure.

We have studied the effect of these sterols on structure and ordering in lipid bilayer membranes using three different types of membrane models, specifically multilamellar dispersions, giant unilamellar vesicles (GUVs), and solid-supported lipid bilayers. Each model system lends itself to be examined quantitatively by certain biophysical techniques, in particular differential-scanning calorimetry, fluorescence microscopy, vesicle-fluctuation analysis, and atomic force microscopy. The membranes were composed of different binary and ternary lipid mixtures with the sterol in question, choosing specific phospholipids, in particular DPPC, POPC, and DOPC, which are known to be relevant for an understanding of many aspects of the generic behavior of biological membranes in relation to lipid domain and raft formation (Marsh, 2013). Importantly, DPPC was chosen because it is a saturated lipid with a high melting point and with both solid and liquid phases in a convenient temperature range for the biophysical experiments. POPC and DOPC were chosen because they are low-melting lipids in fluid states at physiological conditions. Moreover, ternary mixtures with sterols containing both a high- and a low-melting lipid are known to be good model systems of biological membranes (Marsh, 2013) that display coexistence between two liquid phases, the liquid-ordered and the liquid-disordered phase.

In order to study a given physical effect induced by the sterol in question, i.e., phase transition, chain ordering, mechanical membrane properties, or lateral structure, we have chosen a model membrane system, it be multilamellar, GUV, or supported bilayer, with a composition that allows us to study quantitatively the effect in question in the most convenient setting.

2. Materials, model systems, and methods

2.1. Materials

Phospholipids and cholesterol were obtained from Avanti polar lipids (Alabaster, AL). Fucosterol and desmosterol were obtained

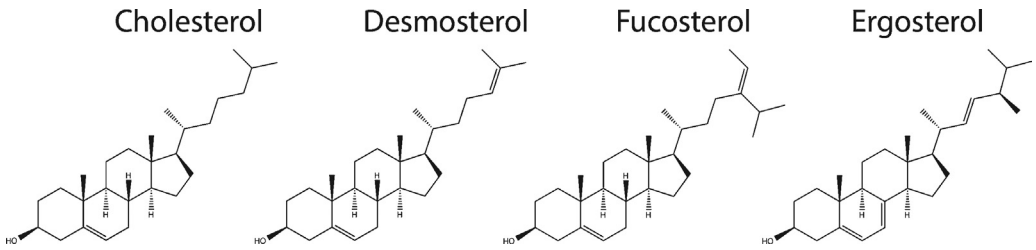

Fig. 1. Structural formulas for higher sterols studied in the present paper: fucosterol, desmosterol, cholesterol, and ergosterol.

from Steraloids (Newport, RI) and ergosterol from Sigma–Aldrich (St. Louis, MO). All lipids where used as received. The fluorescent dyes N-Rh-DPPE was from Avanti polar lipids and LAURDAN was obtained from Invitrogen (Thermo Fisher Scientific, Radnor, PA). Naphtopyrene, solvent, and salts were all from Sigma–Aldrich.

2.2. Model systems and methods

2.2.1. Multilamellar dispersions and DSC

The multilamellar liposome dispersions were prepared by mixing DPPC and the appropriate sterols from chloroform stock solutions. The chloroform was evaporated with a gentle stream of nitrogen and the samples were then placed under reduced pressure overnight. The formed lipid film was hydrated with ultra-pure water by shaking for 30 min at 55 °C.

DSC was performed in a N-DSC II calorimeter (TA instruments, Lindon, UT). A static pressure of 3 atm was applied to prevent bubble formation. A scan rate of 0.5 K/min and a lipid concentration of 5 mM were used. Data was analyzed in Origin 7 (Origin lab, Northampton, MA) and the main phase transition temperature, T_m, was defined from the maximum in the DSC trace.

2.2.2. Preparation of GUVs for fluorescence microscopy

DPPC, DOPC, and sterol stock organic solutions (10 mg/ml) were prepared in chloroform by dissolving the appropriate mass of lipid previously weighed by balance (Mettler Toledo AX205 delta range, $d = 0.01$ mg). The DOPC and DPPC concentrations in the stocks were confirmed by phosphorus analysis (Bartlett, 1959). Sterol concentration was determined by gravimetric analysis. The associated error in the concentration of our stock solutions was $<1\%$. Mixtures containing DOPC, DPPC, and sterol (2:2:1 mol), including the fluorescent probes, were prepared in Cl_3CH/MetOH 2:1 (v/v) (total lipid concentration 0.2 mg/ml). Probes were 0.75 and 0.25 mol% with respect to total lipids for Naphthopyrene and N-Rh-DPPE respectively. In the case of LAURDAN the probe concentration was 1% mol with respect to total lipids. Stock solutions of the fluorescent probes where prepared in Cl_3CH and their concentrations were determined using spectrophotometry. GUVs were prepared following the electroformation method described by Angelova et al. (1992) using a custom-built chamber (Fidorra et al., 2006). Briefly, aliquots of the desired lipid mixture containing the fluorescent probes were deposited on each Pt electrode (4 μl per wire), and the solvent was removed under vacuum for 2 h. After removal of the organic solvent, the chamber was filled with a 200 mM sucrose solution, and an AC field was applied to the chamber using a function generator (Vann Draper Digimess Fg 100, Stenson Derby, UK) with an amplitude of 1.3 V and a frequency of 10 Hz. The electroformation was carried out for 60 min at a temperature of 55 °C for all samples. Subsequently, the GUVs chamber was cooled to room temperature in a time span of approximately 5 h in an oven (J.P. Selecta, Barcelona, Spain) using a temperature ramp (∼0.2 °C/min). The last step was done in order to achieve equilibrium conditions in the samples. Once the solution reached room temperature, the vesicles were transferred to an isoosmolar glucose solution in a special chamber (200 μl of glucose + 50 μl of the GUVs in sucrose in each of the 8 wells of the plastic chamber used (Lab-tek Brand Products, Naperville, IL)). The density difference between the interior and exterior of the GUVs causes the vesicles to sink to the bottom of the chamber, and within a few minutes, the vesicles are ready to be observed using an inverted laser scanning confocal fluorescence microscope. The temperature during image acquisition was controlled to 20.0 ± 0.5 °C.

2.2.3. Laser scanning confocal fluorescence microscopy experiments

Confocal Image stacks were acquired on a Zeiss LSM 510 Meta confocal laser scanning fluorescence microscope. A C-Apochromat 40× water immersion objective with a NA 1.2 was used in our experiments. Two-channel image stacks were acquired using multi-track mode. Argon and NeHe lasers (458 and 543 nm) were used as excitation sources. The laser lines were reflected to the sample through the objective using two different dichroic mirrors (HFT 488/543/633 and HFT 458 for exciting N-Rh-DPPE and Naphthopyrene respectively). The fluorescence emission collected through the objective was directed to the PMT detectors using a mirror. A beam splitter was used to eliminate remnant scattering from the laser sources (NFT 545) in a two-channel configuration. Additional filters were incorporated in front of the PMT detectors in the two different channels to measure the fluorescent intensity, i.e. a long pass filter > 560 nm for N-Rh-DPPE and a band pass filter 500 ± 20 nm for Naphthopyrene. The acquired intensity images were checked to avoid PMT saturation and loss of offsets by carefully adjusting the laser power, the detector gain, and the detector offset. The image stacks were acquired at a sampling rate slightly above the Nyquist frequency, which was calculated to be 40 nm for Δx and Δy and 140 nm for Δz with Huygens Scripting Software (Scientific Volume Imaging, Hilversum, Netherlands). The sampling above the Nyquist frequency was necessary to guarantee sufficient scan speed, which minimizes vesicle movement. The distinct preference of N-Rh-DPPE and Naphthopyrene for disordered and ordered liquid phases respectively was corroborated by comparative experiments using LAURDAN GP (see below).

2.2.4. LAURDAN GP imaging

The main advantages of LAURDAN over many of other fluorescence probes are: (i) the negligible contribution of the probe from the water phase since partitioning into the membrane phase is highly favored, (ii) the even partitioning of LAURDAN in membranes displaying lateral heterogeneity, and (iii) the sensitivity of the probe to lipid packing (e.g., a 50 nm emission shift is observed going from a solid-ordered to a liquid-disordered phase) (Parasassi et al., 1990; Bagatolli, 2006; Bagatolli, 2013). This sensitivity is due to dipolar relaxation processes that occur during the lifetime of the probe (nanoseconds), caused by the presence of water molecules with restricted mobility in the region where LAURDAN is located in the membrane (Parasassi et al., 1990; Bagatolli, 2006; Bagatolli, 2013). Most of the applications of LAURDAN in membranes studies rely on measurements of the generalized polarization (GP) function introduced by Parasassi et al. (1990) as an analytical method to quantitatively determine the relative amount of coexisting phases in a membrane as well as to study their temporal fluctuations. The GP function shows very characteristic values depending on the membrane phase state (Bagatolli, 2006, 2013). For instance, in the solid-ordered phase the observed GP values are around 0.6 (the extent of solvent relaxation in the nanosecond regime is very low) whereas for the liquid-disordered phase the values are below 0.15, often down to negative values around −0.2 depending on the temperature (here the extent of solvent relaxation in the nanosecond regime is high). The liquid-ordered phase show intermediate GP values depending on the cholesterol molar fraction in the membrane, which in turn is related to the hydration properties of the membrane (Dietrich et al., 2001).

LAURDAN GP measurements were here performed on a custom-build microscope setup on a specially constructed Olympus IX70 microscope. The objective used was a 60× water objective with an NA of 1.2. The excitation light source was a femtosecond Ti:Sa laser (HP Mai Tai, tunable excitation range 690–960 nm, Spectra Physics, Mountain View, CA) and the excitation wavelength was 780 nm. The fluorescence signals were collected in two separate detectors

(I_B and I_R), equipped with band passes of 446 ± 23 nm and 492 ± 23 nm, respectively. LAURDAN GP values were calculated using the following equation: $GP = (I_B - I_R)/(I_B + I_R)$, where I_B and I_R are the fluorescence intensities measured in the blue and red edges of the LAURDAN fluorescence emission spectrum. Corrections using the G factor were performed in our experiments as previously reported (Brewer et al., 2010). The average GP values for liquid-ordered and liquid-disordered phases were computed from the analysis of approximately 20 vesicles.

2.2.5. GUVs and vesicle fluctuation analysis

GUVs were formed by the electroformation technique (Angelova et al., 1992). After having been detached from the electrodes at the end of the preparation protocol, the GUVs were observed directly in the electroformation cuvette (for details of the protocol, see also Section 2.2.2). A temperature-controlled chamber holder (25 °C) was used to maintain constant temperature. The giant vesicles were visualized using a phase contrast microscope (Axiovert S100 Zeiss, Göttingen, Germany) equipped with an ×40/0.60 objective (440865 LD Achroplan). The vesicle two-dimensional contour in the focal plane of the objective was thus obtained, and a CCD Camera (SONY SSC-DC50AP) was used to record series of 10,000–45,000 pictures at a rate of 25 frames per second with a video integration time of 4 ms.

The video image sequences of the thermal fluctuations of the GUVs were analyzed using custom-made software to perform contour extraction, contour cleaning, and the fluctuation-analysis procedures presented in Ipsen et al. (2017). The analysis of the statistical distribution of vesicle contours based on a mode decomposition of the angular correlation function introduced in Henriksen et al. (2004) was performed. Static analysis of the flicker spectrum led to the determination of the bending modulus by analysis of the distributions of the amplitudes of decomposition of the angular correlation function in the Legendre polynomial basis.

2.2.6. Supported bilayers and atomic force microscopy (AFM)

Single- and double-supported bilayers on mica were prepared using the spincoating method (Simonsen and Bagatolli, 2004) and following the protocol detailed in Jensen et al. (2007). Briefly, dry lipid films on mica were prepared by spincoating a 10 mM lipid (total) stock containing 0.5% of a fluorescent dye ($DiIC_{18}$) in hexane/methanol (97:3 volume ratio) onto freshly cleaved mica. The sample was stored in vacuum for 10–15 h and was subsequently hydrated in 150 mM NaCl aqueous solution at 55 °C for 1 h. The hydrated sample was placed in an epi-fluorescence microscope, and rinsed with hot hydration solution to fabricate areas with single- and double-supported lipid bilayers and to eliminate bilayer fragments floating in solution. Following cooling to ambient temperature, the lipid bilayer undergoes phase separation and coarsening.

Atomic force microscopy on the first (proximal) bilayer was performed using a JPK Nanowizard AFM system (JPK Instruments, Berlin, Germany) operated in contact mode. Silicon nitride cantilevers of the type (MSCT, C-lever, Bruker) were used, with a nominal spring constant of 0.01 N/m and a resonance frequency of 7 kHz. During scanning, the sample was located in the fluid cell (JPK) also used for fluorescence imaging. Images were analyzed with SPIP (Image Metrology, Hørsholm, Denmark).

Fluorescence microscopy was also performed on the supported membranes using a Nikon TE2000 microscope with a 40× objective (Nikon, ELWD, Plan Fluor, NA = 0.6). Fluorescence excitation was done with a halogen lamp and using a G-2A (Nikon) filtercube for the $DiIC_{18}$ probe. Images were recorded with an EM-CCD camera (Sensicam em, PCO-Imaging, Kelheim, Germany) and operated with Camware software (PCO).

3. Results

3.1. Sterols suppress the lipid phase transition

In Fig. 2 are shown the thermograms with the specific heat as a function of temperature for binary mixtures of DPPC with different sterols. The sharp peak for pure DPPC around 42 °C signals the main phase transition (solid-ordered to liquid-disordered). As increasing amounts of sterols are incorporated, the transition broadens into a two-phase coexistence region below the pure DPPC melting point, demonstrating that all sterols are more soluble in the liquid phase than in the solid phase. The maximum of the specific heat main peaks is taken as a measure of a midpoint transition temperature, T_m. By comparison of the variation of T_m as a function of sterol concentration for the four different sterols as shown in Fig. 3. It can be concluded that the effect of the sterols with respect to suppressing the phase transition increases progressively in the order fucosterol > desmosterol > ergosterol > cholesterol.

A determination of the full phase diagram for binary lipid mixtures with sterols like cholesterol and ergosterol is known to be a very delicate matter (Mouritsen and Zuckermann, 2004). We have therefore not attempted to construct a thermodynamic phase diagram for the desmosterol and fucosterol systems. However, since we are here mainly interested in the differential effect of the ordering capacity of the higher sterols, the present thermal analysis suffices to suggests that the algae sterols are substantially poorer to order disordered (fluid) lipid chains than cholesterol and ergosterol, and conversely they are better to disorder ordered lipid chains.

3.2. Desmosterol and fucosterol are poor membrane-stiffening agents

In Fig. 4 is shown a phase contrast image of a GUV composed of POPC with 20% fucosterol at 25 °C. Clearly fluctuations make the shape of the vesicle deviate from spherical form. The estimated bending elastic modulus calculated from the analysis is represented an average of measurements amongst a populations respectively of 10 vesicles (4:1 POPC:fucosterol) and 7 vesicles (4:1 POPC:demosterol), whose diameters were in the range 30–60 μm. The following values were obtained

$\kappa = (51.9 \pm 0.9) k_B T$ for fucosterol.
$\kappa = (65.9 \pm 0.8) k_B T$ for desmosterol.

The bending modulus for pure POPC vesicles is $\kappa = (38.5 \pm 0.8)$ $k_B T$ (Henriksen et al., 2004), for POPC with 20% ergosterol, $\kappa = (53.5 \pm 1.7) k_B T$, and for POPC with 20% cholesterol, $\kappa = (70.2 \pm 0.8) k_B T$ (Henriksen et al., 2004), suggesting the following order of sterols for their capacity to increase the bending modulus, cholesterol > desmosterol > ergosterol > fucosterol.

3.3. Fucosterol and desmosterol are poorer ordering agents than cholesterol

As previously reported for cholesterol-containing ternary mixtures (Baumgart et al., 2007; Sezgin et al., 2012), the fluorescent probes N-Rh-DPPE and Naphtopyrene (Fig. 5a) show favorable partitioning into the liquid-disordered and liquid-ordered phases, respectively. In Fig. 5b are shown the fluorescence microscope images of GUVs composed of DOPC:DPPC:sterol mixtures (2:2:1 mol) labeled with these two fluorescent probes.

Two key observations can be made from the confocal fluorescence images. First, although N-Rh-DPPE systematically label one region of the membrane, Napthopyrene show a different behavior depending on which sterol is used in the mixture. In the case of cholesterol, there is a clear separation between the two

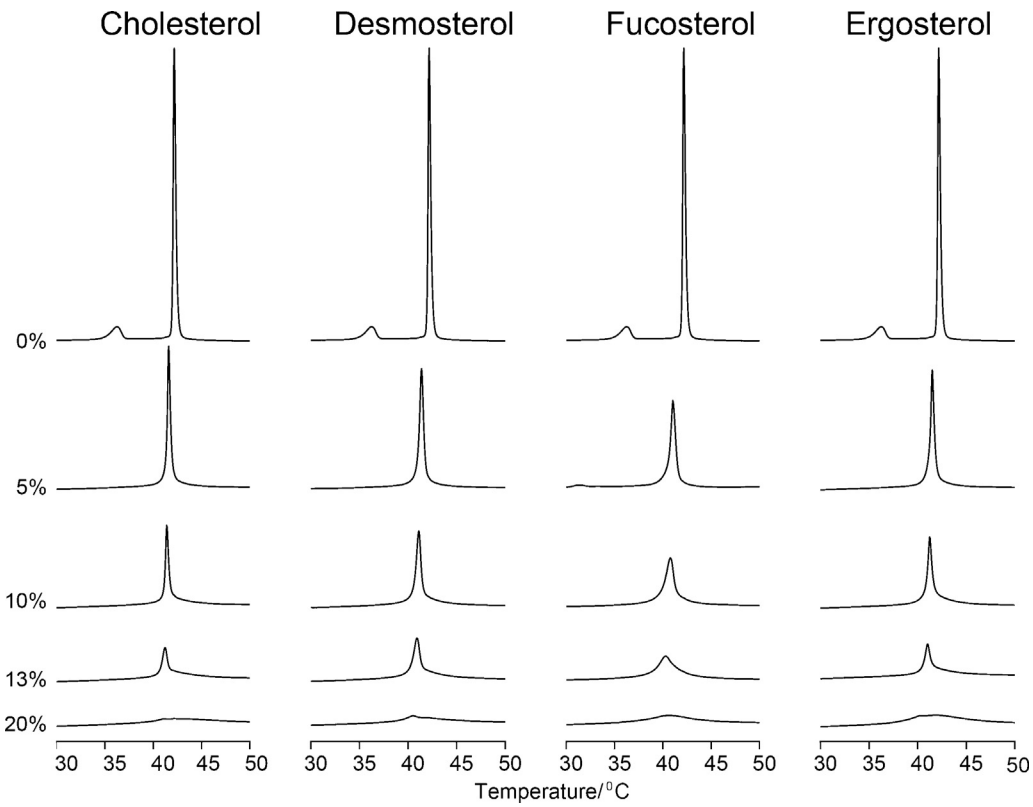

Fig. 2. Thermograms showing the excess specific heat as a function of temperature for multilamellar dispersions of mixtures of DPPC with four different higher sterols at varying concentrations.

probes labeling each of the different phases separately. In the case of desmosterol, the partition of Napthopyrene become more even between the coexisting regions, while for fucosterol both probes co-localize almost evenly in the coexisting membrane regions.

This variable partitioning of the probes demonstrated in Fig. 5b is in line with previous observations done in other lipid mixtures, where each probe's partitioning properties among different membrane regions are highly dependent on the local chemical composition of the membrane domain and not on the actual phase state (Bagatolli, 2006; Bagatolli and Gratton, 2000a, 2000b; Juhasz et al., 2010, 2012). Hence, these images cannot be used to assign lipid phases to the systems, but only determine the sensitivity of the probe's partition information to infer differences between the coexisting lipid domains. In all the images in Fig. 5b we observed rounded domains, indicating that the domains are controlled by an isotropic line tension that is characteristic of liquid phases. However, comparing with the cholesterol-containing mixtures, the shape of the domains progressively elongates in the order cholesterol < desmosterol < fucosterol. Taking all these results into account, we suggest that the three sterols possess different capacities to influence the coexisting liquid phases.

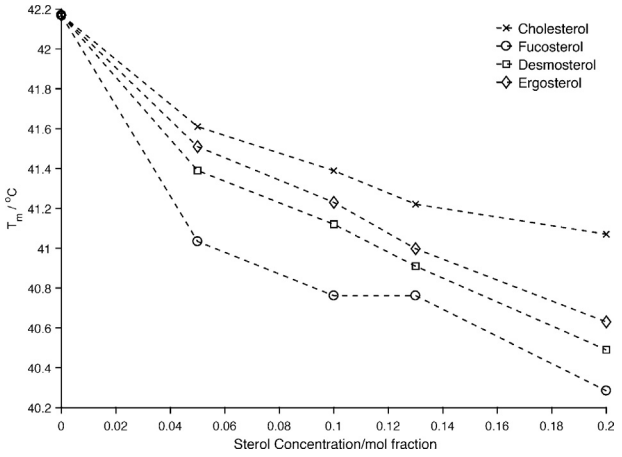

Fig. 3. Transition temperatures, T_m, extracted from the peak positions of the specific heat in the thermograms shown in Fig. 2. The data refer to measurements on single samples. The estimated uncertainty is ±0.1 degree.

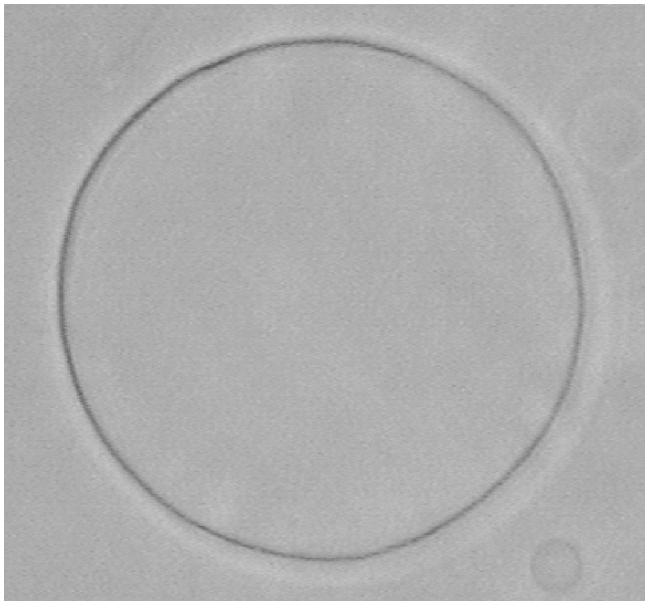

Fig. 4. Phase contrast microscopy image of a GUV composed of POPC with 20% fucosterol at 25 °C. Fluctuations away from spherical shape is seen.

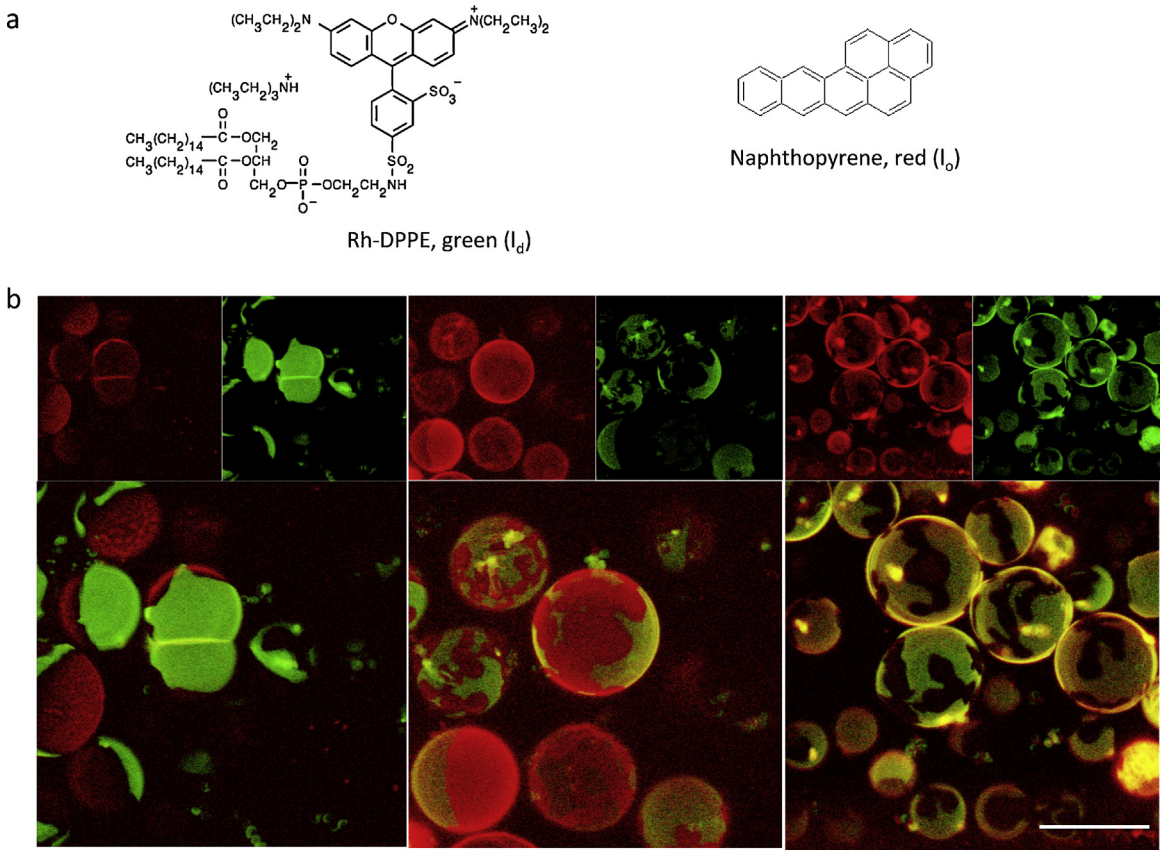

Fig. 5. (a) Structural formulas for the two probes, N-Rh-DPPE and Naphtopyrene, used to distinguish liquid-disordered and liquid-ordered phases in lipid bilayers. (b) Confocal fluorescence microscope images of GUVs made of mixtures of DOPC/DPPC/sterol (2:2:1) for three different sterols at 20 °C showing the contribution of the two different channels (top) and the overlay (bottom). Scale bar correspond to 30 μm. Left: cholesterol; middle: desmosterol; and right: fucosterol.

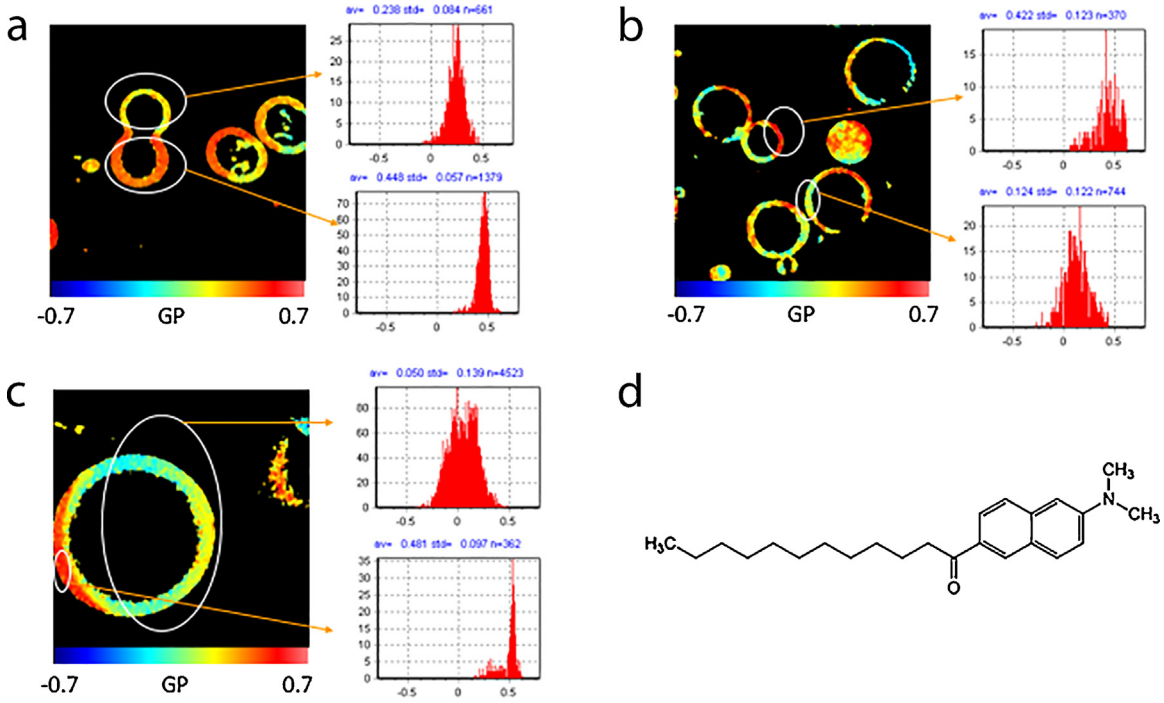

Fig. 6. LAURDAN GP images (a–c) of GUVs composed of mixtures of DOPC/DPPC/sterol (2:2:1) for three different sterols (i.e., cholesterol, desmosterol, and fucosterol) at 20 °C. Representative generalized polarization (GP) images of GUVs are shown along with corresponding GP histograms. Molecular structure (d) of the fluorescent lipid-analog probe LAURDAN.

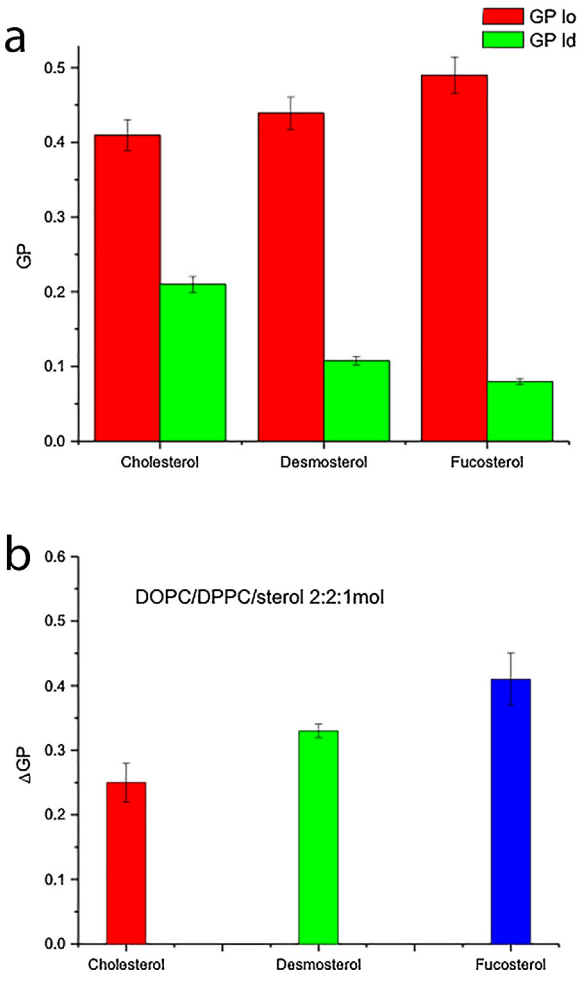

Fig. 7. (a) LAURDAN generalized polarization (GP) average values for liquid-ordered (lo) and liquid-disordered (ld) phases computed from GUVs composed of mixtures of DOPC/DPPC/sterol (i.e., cholesterol, desmosterol, and fucosterol) at 2:2:1 mol ratio. (b) Difference, ΔGP, in generalized polarization for lo and the ld phase, respectively. All data refer to 20 °C.

A more rigorous assessment of the nature of the coexisting phases and the ordering capacity of the sterols can be gauged from generalized polarization (GP) data using LAURDAN (Fig. 6d) as a fluorescent probe. LAURDAN offers the advantage of performing a quantitative analysis, which is different from the qualitative data provided by Napthopyrene and N-Rh-DPPE imaging. As stated earlier LAURDAN is evenly distributed in membranes displaying coexisting phases and its fluorescence signal is dependent on the water dipolar relaxation near the lipid head groups, which in turn is sensitive to the degree of order of the lipid acyl chains (Bagatolli, 2006, 2013). Single GUVs with two different phases are clearly highlighted by the difference in LAURDAN GP in the two coexisting regions as shown in Fig. 6a–c, implying that the two phases can readily be singled out on the level of single GUVs.

The histograms for the GP function measured by two-photon fluorescence are also shown in Fig. 6a–c. The corresponding averages of the GP values in Fig. 7a show that in all cases the more ordered domains correspond to GP values previously obtained for liquid ordered-phases in mixtures displaying fluid immiscibility (Dietrich et al., 2001), i.e., values that are different from those observed for the coexistence of fluid-disordered/solid-ordered (gel) phases (Bagatolli and Gratton, 2000a, 2000b). In addition the data clearly demonstrate that the liquid-disordered phase gets less ordered in the sequence cholesterol > desmosterol > fucosterol, and the liquid-ordered phase gets slightly more ordered along the same sequence. The combination of these effects is most clearly seen in the difference in generalized polarization, ΔGP = GP(liquid-ordered) – GP(liquid-disordered), as shown in Fig. 7b.

The conclusion from all these measurements (Napthopyrene/N-Rh-DPPE confocal fluorescence and LAURDAN GP imaging) is that cholesterol, desmosterol, and fucosterol all induce liquid immiscibility in mixtures with DOPC and DPPC. Additionally, fucosterol and desmosterol induce acyl-chain order in liquid membranes, but less effectively than cholesterol in the order: cholesterol > desmosterol > fucosterol, possibly reflecting the impact of the different molecular structure of the sterols in the lateral structure of the membrane.

3.4. Fucosterol and desmosterol promote liquid–liquid immiscibility and domain formation

In Fig. 8 are shown visualizations of the lateral structure of solid-supported lipid bilayers composed of ternary mixtures DOPC:DPPC:sterol (2:2:1) with fucosterol and desmosterol, respectively. The bilayers contain 0.5% of a fluorescent dye ($DiIC_{18}$) that dissolves predominantly in liquid-disordered phases. Images are shown as obtained by both AFM and fluorescence microscopy. Both types of imaging techniques demonstrate that at 22 °C either sterol is capable of inducing liquid–liquid immiscibility and a lateral membrane structure that is composed of lipid domains.

The double-supported membrane configuration provides a convenient control for the effect of the solid support on the domain pattern. The distal bilayer is interacting more weakly with the solid support than the proximal bilayer and as a result, domains coarsening and relaxations in the domain shape will be less restricted in the distal bilayer.

It is likely that the two phases in the images in Fig. 8 are respectively a sterol-rich liquid-ordered phase and a sterol-poor liquid-disordered phase. The topography scans of the proximal bilayer in Fig. 8 show that the height difference between the domains is about 0.6–0.8 nm as typically observed for two fluid membranes phases (Jensen et al., 2007). Within the level of accuracy of the present measurements it is not possible to discern any variation in this height difference for the fucosterol and desmosterol systems. However, we notice that the measured height difference is clearly below the AFM height difference of ~1.2 nm measured for the same lipids (DOPC:DPPC, 1:1) without sterols (Dreier et al., 2014) suggesting a liquid nature of both membrane phases.

The liquid nature of the lipid domains is also supported by the finding of rounded interfaces both in the fluorescence and AFM images, suggesting that the lateral organization is controlled by an isotropic line tension.

4. Discussion

We have in this paper chosen the lipid composition of the model systems in question, it be multilamellar, GUV, or supported bilayer, to allow us in the most reliable and quantitative setting to investigate the effect of sterols on a variety of physico-chemical membrane properties, such as phase transition temperature, chain ordering, mechanical bending modulus, and lateral structure. Whereas we have used DOPC for most of our models systems, it is more convenient to use POPC for forming stable GUVs for vesicle fluctuation analysis (Henriksen et al., 2004). We are fully aware that the POPC/DPPC/chol ternary mixture does impose a general experimental challenge for the membrane biophysicists to study phase separation in GUVs, in that older work (Feigenson, 2007) has postulated that mixtures with POPC and DOPC in raft mixtures display different phase behavior. However, more recent work by

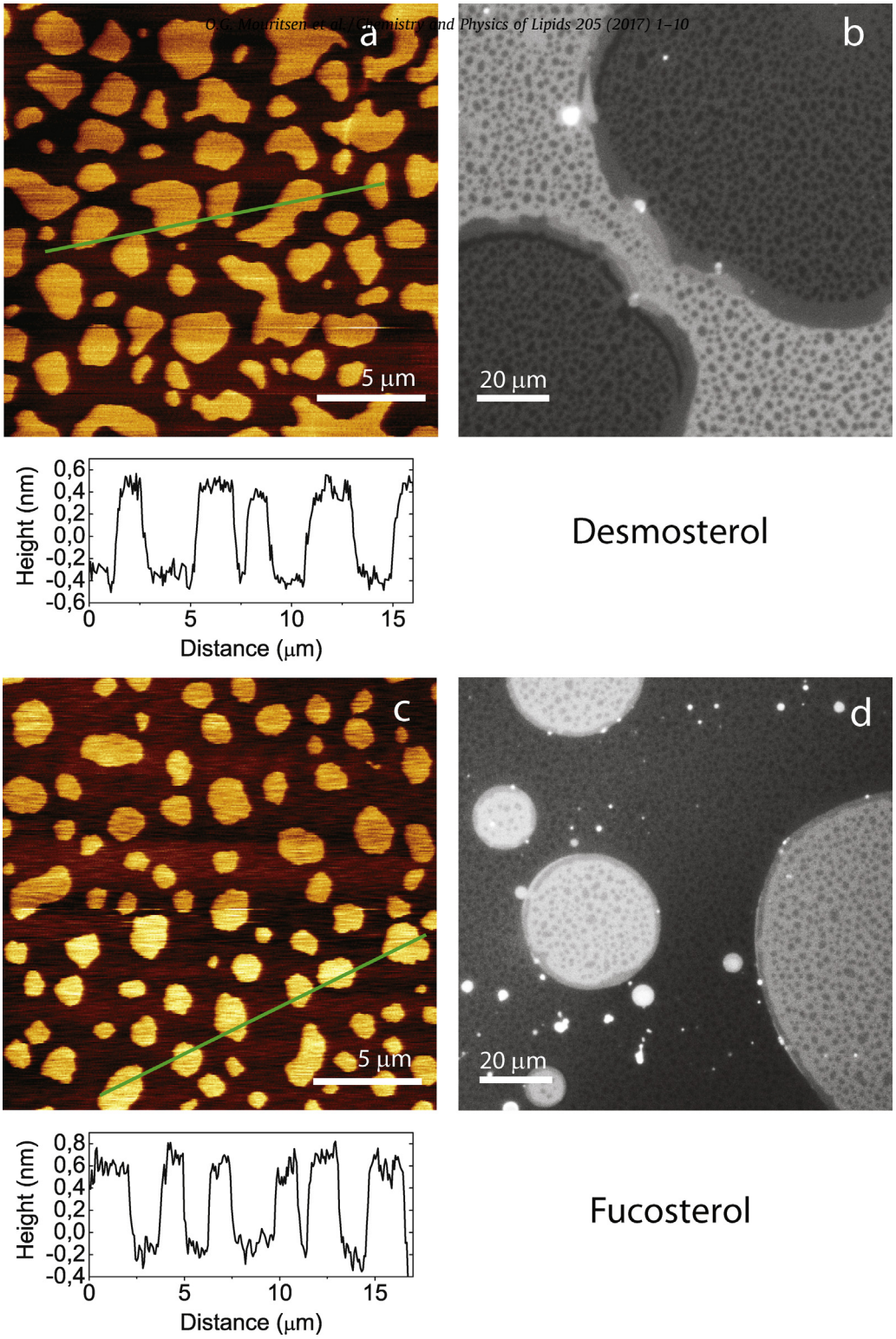

Fig. 8. Solid-supported bilayers with composition DOPC:DPPC:sterol (2:2:1) at 22 °C. AFM topography scans of the lowest (proximal) bilayer are shown in (a,c) and corresponding fluorescence microscopy images in (b,d). Results for fucosterol are shown in (a,b) and results for desmosterol in (c,d). Topography profiles across domains are shown corresponding to the green lines in the AFM images. The large bright areas in the fluorescence images are regions containing double supported bilayers and darker areas are regions with one bilayer.

the same group (Heberle et al., 2010) corrected this statement, providing evidence that mixtures with both DOPC and POPC display a very similar phase coexistence of liquid-ordered and liquid-disordered domains (phases). This has also been discussed in detail by Marsh (2013). Hence, there is a consensus among workers in the field, that both DOPC and POPC are good representatives for a low-melting lipid in models of membranes with cholesterol (Marsh, 2009). We have assumed that the same is the case for other higher sterols, like desmosterol and fucosterol.

Although only indirect information of lipid acyl chain ordering, the variation of the midpoint transition temperature T_m measured by calorimetry shown in Fig. 3 suggests that the various sterols

disorder acyl chains in solid-ordered phase in the sequence cholesterol < ergosterol < demosterol < fucosterol. This is consistent with our finding from fluorescence microscopy and GP polarization data that clearly demonstrate that the liquid-disordered phase becomes more ordered in the sequence cholesterol > desmosterol > fucosterol, and the liquid-ordered phase gets slightly less ordered along the same sequence. Comparison of micromechanics data for bending and area-expansion moduli with ^{2}H NMR data for acyl chain ordering (Henriksen et al., 2006) in sterol-containing POPC bilayers has shown that there is a universal relationship between membrane mechanical parameters and acyl chain ordering. Based on this and earlier work on ergosterol (Henriksen et al., 2004) our finding in Section 3.2 of an increasing bending modulus of liquid-disordered bilayers in the order cholesterol > desmosterol > ergosterol > fucosterol is consistent with data from both calorimetry in Fig. 3 and GP polarization measurements in Fig. 7.

Whereas the micromechanical results shed some light on the differential ability of the different sterols for ordering fluid lipid phases and domains, the present GP data does not provide sufficient information to discriminate between sterol partitioning into coexisting domains and ability to induce order at the molecular level. It could very well be that the relative sterol partitioning into both phases may impact on the difference in the ΔGP measured, considering that this is only an indirect measure of the lipid order since GP basically measures the extent of water dipolar relaxation between the two coexisting phases. Further insight into this problem would require measurement of the molar fraction of the sterols in the coexisting phases in the ternary mixture, e.g., by NMR methods (Orädd et al., 2005), which in turn requires knowledge of the full ternary phase diagram.

The observation of rounded (liquid-ordered) lipid domains in both fluorescence and AFM imaging, Figs. 5 and 8, respectively, suggests that the domains are controlled by an isotropic line tension that is characteristic of liquid phases, although their shapes depend on the sterol in question with elongation in the order cholesterol < desmosterol < fucosterol, suggesting that the three sterols possess different capacities to influence the coexisting liquid phases. Further testimony to the fact that the algal sterols desmosterol and fucosterol fluidize solid-ordered lipid bilayers is furnished by the AFM imaging in Fig. 8 which clearly shows that the bilayer thickness in the presence of the sterols is below that of the same lipid bilayer without sterols (Dreier et al., 2014).

A number of recent studies have been concerned with the question as to which molecular property of the different higher sterols has the major influence on their capacity to influence ordering in lipid bilayer membranes (Vilchèze et al., 1996; Bittman, 1997; Miao et al., 2002; Huster et al., 2005; Bacia et al., 2005; Shahedi et al., 2006; Vainio et al., 2006; Megha and Erwin London, 2006; Samuli et al., 2007; Mannock et al., 2010; Shaghaghi et al., 2016), and some of this work has addressed the question whether cholesterol can be replaced by some of the other higher sterols. Currently there is no clear consensus and it appears that there is a subtle interplay between the effect of the structure and degree of saturation of the side chain and the number of double bonds at the fused ring structure. With regard to the capacity for ordering fluid acyl lipid chains it appears that it is the structure of the side chain that is of more importance (Shaghaghi et al., 2016), which in turn is responsible for the tilt of the sterol molecule when imbedded in the lipid bilayer (Aittoniemi et al., 2006). The data presented in the present paper is consistent with this picture.

5. Conclusion

The present paper provide additional support to the hypothesis (Nielsen et al., 2000; Miao et al., 2002) that one of the crucial traits of the higher sterols, despite their chemical difference across the different biological kingdoms, is that they share a common capacity to influence lipid chain order and lateral organization of membranes in a special way that lead to formation of liquid-ordered phases. This is in contrast to the common evolutionary precursor lanosterol in the biochemical pathway to the higher sterols, which is unable to stabilize liquid-ordered phases (Miao et al., 2002; Róg et al., 2008).

A major finding of the present work is, that the two algal higher sterols desmosterol and fucosterol, similarly to cholesterol, ergosterol, phytosterols from animals, fungi, and higher plants respectively, are capable of inducing a liquid-ordered phase in bilayer membranes, hence lending further support to the hypothesis that the presence of membrane states or domains of a liquid-ordered nature is a common trait of the plasma membranes of higher organisms (Bloom and Mouritsen, 1995; Nielsen et al., 2000; Miao et al., 2002; Mouritsen and Zuckermann, 2004).

Acknowledgements

Part of this work was supported by a grant from Lundbeckfonden (R95-A10447).

References

Aittoniemi, J., Róg, T., Niemelä, P., Pasenkiewicz-Gierula, M., Karttunen, M., Vattulainen, I., 2006. Tilt: major factor in sterols' ordering capability in membranes. J. Phys. Chem. B 110, 25562–25564.
Almeida, P., 2014. The many faces of lipid rafts. Biohys. J. 106, 1841–1843.
Almeida, P., Loura, L.M., Fedorov, A., Prieto, M., 2005. Lipid rafts have different sizes depending on membrane composition: a time-resolved fluorescence resonance energy transfer study. J. Mol. Biol. 346, 1109–1120.
Alsop, R.J., Maikel, C., Rheinstädter, M.C., 2016. Lipid rafts in binary lipid/cholesterol bilayers. In: Catalá, A. (Ed.), Membrane Organization and Lipid Rafts in the Cell and Artificial Membranes. Nova, Series on Cell Biology Research Progress, , pp. 17–42.
Angelova, M.I., Soléau, S., Méléard, P., Faucon, F., Bothorel, P., 1992. Preparation of giant vesicles by external AC fields. Kinetics and applications. Prog. Coll. Polym. Sci. 89, 127–131.
Armstrong, C.L., Marquardt, D., Dies, H., Kučerka, N., Yamani, Z., Harroun, T.A., Katsaras, J., Shi, A.C., Rheinstädter, M.C., 2013. The observation of highly ordered domains in membranes with cholesterol. PLoS ONE 8, e66162.
Bezlyepkina, N., Gracia, R.S., Shchelokovskyy, P., Lipowsky, R., Dimova, R., 2013. Phase diagram and tie-line determination for the ternary mixture DOPC/eSM/cholesterol. Biophys. J. 104, 1456–1464.
Bacia, K., Schwille, P., Kurzchalia, T., 2005. Sterol structure determines the separation of phases and the curvature of the liquid-ordered phase in model membranes. Proc. Natl. Acad. Sci. U. S. A. 102, 3272–3277.
Bagatolli, L.A., 2006. To see or not to see: lateral organization of biological membranes and fluorescence microscopy. Biochim. Biophys. Acta 1758, 1541–1556.
Bagatolli, L.A., 2013. LAURDAN fluorescence properties in membranes: a journey from the fluorometer to the microscope. In: Mely, Y., Duportail, G. (Eds.), Fluorescent Methods to study Biological Membranes, Springer Series on Fluorescence, vol. 13. , pp. 3–36.
Bagatolli, L.A., Gratton, E., 2000a. A correlation between lipid domain shape and binary phospholipid mixture composition in free standing bilayers: a two-photon fluorescence microscopy study. Biophys. J. 79, 434–447.
Bagatolli, L.A., Gratton, E., 2000b. Two photon fluorescence microscopy of coexisting lipid domains in giant unilamellar vesicles of binary phospholipid mixtures. Biophys. J. 78, 290–305.
Bagatolli, L.A., Ipsen, J.H., Simonsen, A.C., Mouritsen, O.G., 2010. A new outlook on organization of lipids in membranes: searching for a realistic connection with the organization of biological membranes. Prog. Lip. Res. 49, 378–389.
Bartlett, G.R., 1959. Phosphorus assay in column chromatography. J. Biol. Chem. 234, 466–468.
Beck, J.G., Mathieu, D., Loudet, C., Buchoux, S., Dufourc, E.J., 2007. Plant sterols in "rafts": a better way to regulate membrane thermal shocks. FASEB J. 21, 1714–1723.
Baumgart, T., Hunt, G., Farkas, E.R., Webb, W.W., Feigenson, G.W., 2007. Fluorescence probe partitioning between Lo/Ld phases in lipid membranes. Biochim. Biophys. Acta 1768, 2182–2194.
Bittman, R., 1997. Has nature designed the cholesterol side chain for optimal interaction with phospholipids? Subcell. Biochem. 28, 145–171.
Bloom, M., Mouritsen, O.G., 1995. The evolution of membranes. In: Lipowsky, R., Sackmann, E. (Eds.), Handbook of Biological Physics, vol. 1. , pp. 65–95.

Brewer, J., Bernardino de la Serna, J., Wagner, K., Bagatolli, L.A., 2010. Multiphoton excitation fluorescence microscopy in planar membrane systems. Biochim. Biophys. Acta 1798, 1301–1308.

Dai, M.C., Chiche, H.B., Düzgünes, N., Ayanoglu, E., Djerassi, C., 1991. Phospholipid studies of marine organisms: 26. Interactions of some marine sterols with 1-stearoyl-oleoyl phosphatidylcholine (SOPC) in model membranes. Chem. Phys. Lipids 59, 245–253.

Davis, J.H., Clair, J.J., Juhasz, J., 2009. Phase equilibria in DOPC/DPPC-d_{62}/cholesterol mixtures. Biophys. J. 96, 521–539.

Davis, J.H., Ziani, L., Schmidt, M.L., 2013. Critical fluctuations in DOPC/DPPC-d_{62}/cholesterol mixtures: ^{2}H magnetic resonance relaxation. J. Chem. Phys. 139, 045104.

Dietrich, C., Bagatolli, L.A., Volovyk, Z.N., Thompson, N.L., Levi, M., Jacobson, K., Gratton, E., 2001. Lipid rafts reconstituted in model membranes. Biophys. J. 80, 1417–1428.

Dreier, J., Brewer, J., Simonsen, A.C., 2014. Systematic variation of gel-phase texture in phospholipid membranes. Langmuir 30, 10678–10685.

Garvik, O., Benediktson, P., Simonsen, A.C., Ipsen, J.H., Wüstner, D., 2009. The fluorescent cholesterol analog dehydroergosterol induces liquid-ordered domains in model membranes. Chem. Phys. Lipids 159, 114–118.

Feigenson, G.W., 2007. Phase boundaries and biological membranes. Annu. Rev. Biophys. Biomol. Struct. 36, 63–77.

Feigenson, G.W., Buboltz, J.T., 2001. Ternary phase diagram of dipalmitoyl-PC/dilauroyl-PC/cholesterol: nanoscopic domain formation driven by cholesterol. Biophys. J. 80, 2775–2788.

Fidorra, M., Duelund, L., Simonsen, A.C., Bagatolli, L.A., 2006. Absence of fluid-ordered/fluid-disordered phase coexistence in ceramide/POPC mixtures containing cholesterol. Biophys. J. 90, 4437–4451.

Grosjean, K., Mongrand, S., Beney, L., Simon-Plas, F., Gerbeau-Pissot, P., 2015. Differential effect of plant lipids on membrane organization specificities of phytosphingolipids and phytosterols. J. Biol. Chem. 290, 5810–5825.

Heberle, F.A., Wu, J., Goh, S.L., Petruzielo, R.S., Feigenson, G.W., 2010. Comparison of three ternary lipid bilayer mixtures: FRET and ESR reveal nanodomains. Biophys. J. 99, 3309–3318.

Henriksen, J., Rowat, A., Ipsen, J.H., 2004. Vesicle fluctuation analysis of the effects of sterols on membrane bending rigidity. Eur. Biophys. J. 33, 732–741.

Henriksen, J.H., Rowat, A.C., Brief, E., Hsueh, Y.-W., Thewalt, J.L., Zuckermann, M.J., Ipsen, J.H., 2006. Universal behavior of membranes with sterols. Biophys. J. 90, 1639–1649.

Hodzic, A., Rappolt, M., Amenitsch, H., Laggner, P., Pabst, G., 2008. Differential modulation of membrane structure and fluctuations by plant sterols and cholesterol. Biophys. J. 94, 3935–3944.

Hsueh, Y.W., Gilbert, K., Trandum, C., Zuckermann, M.J., Thewalt, J., 2005. The effect of ergosterol on dipalmitoylphosphatidylcholine bilayers: a deuterium NMR and calorimetric study. Biophys. J. 88, 1799–1808.

Hsueh, Y.-W., Chen, M.-T., Patty, P.J., Code, C., Cheng, J., Frisken, B.J., Zuckermann, M. J., Thewalt, J., 2007. Ergosterol in POPC membranes: physical properties and comparison with structurally similar sterols. Biophys. J. 92, 1606–1615.

Huster, D., Scheidt, H.A., Arnold, K., Hermann, A., Müller, P., 2005. Desmosterol may replace cholesterol in lipid membranes. Biophys. J. 88, 1838–1844.

Ilias, A.M., Conner, W.E., Lin, D.S., Ahmad, M.U., 2006. Sterol composition of some seaweeds. Eur. J. Lipid Sci. Technol. 87, 345–346.

Ipsen, J.H., Mouritsen, O.G., Karlström, G., Wennerström, H., Zuckermann, M.J., 1987. Phase equilibria in the lecithin-cholesterol system. Biochim. Biophys. Acta 905, 162–172.

Ipsen, J.H., Hansen, A.G., Bathia, T., 2017. Vesicle fluctuation analysis. In: Dimova, R., Marques, C. (Eds.), The Giant Vesicle Book. CRC Press, Boca Raton.

Jacobson, K., Mouritsen, O.G., Anderson, G.W., 2007. Lipid rafts at a cross road between cell biology and physics. Nat. Cell Biol. 9, 7–14.

Jensen, M.H., Morris, E.J., Simonsen, A.C., 2007. Domain shapes, coarsening, and random patterns in ternary membranes. Langmuir 23, 8135–8141.

Juhasz, J., Davis, J.H., Sharom, F.J., 2010. Fluorescent probe partitioning in giant unilamellar vesicles of 'lipid raft' mixtures. Biochem. J. 430, 415–423.

Juhasz, J., Davis, J.H., Sharom, F.J., 2012. Fluorescent probe partitioning in GUVs of binary phospholipid mixtures: implications for interpreting phase behavior. Biochim. Biophys. Acta 1818, 19–26.

Konyakhina, T.M., Wu, J., Mastroianni, J.D., Heberle, F.A., Feigenson, G.W., 2013. Phase diagram of a 4-component lipid mixture: DSPC/DOPC/POPC/chol. Biochim. Biophys. Acta 1828, 2204–2214.

Mannock, D.A., Lewis, R.N.A.H., McCullen, T.P.W., McElhaney, R.N., 2010. The effect of variations in phospholipid and sterol structure on the nature of lipid–sterol interactions in lipid bilayer model membranes. Chem. Phys. Lipids 163, 403–448.

Marsh, D., 2009. Cholesterol-induced fluid membrane domains: a compendium of lipid-raft ternary phase diagrams. Biochim. Biophys. Acta 1788, 2114–2123.

Marsh, D., 2013. CRC Handbook of Lipid Bilayers. CRC Press, Boca Raton, FL.

Megha, O.B., Erwin London, E., 2006. Cholesterol precursors stabilize ordinary and ceramide-rich ordered lipid domains (lipid rafts) to different degrees. J. Biol. Chem. 281, 21903–21913.

Miao, L., Nielsen, M., Thewalt, J., Ipsen, J.H., Bloom, M., Zuckermann, M.J., Mouritsen, O.G., 2002. From lanosterol to cholesterol: structural evolution and differential effects on lipid bilayers. Biophys. J. 82, 1429–1444.

Mouritsen, O.G., 2010. The liquid-ordered state comes of age. Biochim. Biophys. Acta 1798, 1286–1288.

Mouritsen, O.G., 2011. Model answers to membrane questions. Cold Spring Harb. Perspect. Biol. 3, 33–47.

Mouritsen, O.G., Bagatolli, L.A., 2016. Life – As Matter of Fat: Lipids in a Membrane Biophysics Perspective. Springer, New York.

Mouritsen, O.G., Zuckermann, M.J., 2004. What's so special about cholesterol? Lipids 39, 1101–1113.

Nielsen, M., Thewalt, J., Miao, L., Ipsen, J.H., Bloom, M., Zuckermann, M.J., Mouritsen, O.G., 2000. Sterol evolution and the physics of membranes. Europhys. Lett. 52, 368–374.

Orädd, G., Westerman, P.W., Lindblom, G., 2005. Lateral diffusion coefficients of separate lipid species in a ternary raft-forming bilayer: a Pfg-NMR multinuclear study. Biophys. J. 89, 315–320.

Patterson, G.W., 1991. Sterols of algae. In: Pattersen, G.W., Nes, W.D. (Eds.), Physiology and Biochemistry of Sterols. American Oil Chemists' Society, Champaign, IL, USA, pp. 118–157.

Parasassi, T., De Stasio, G., d'Ubaldo, A., Gratton, E., 1990. Phase fluctuation in phospholipid membranes revealed by Laurdan fluorescence. Biophys. J. 57, 1179–1186.

Rheinstädter, M.C., Mouritsen, O.G., 2013. Small-scale structure in fluid cholesterol-lipid bilayers. Curr. Opin. Colloid Int. Sci. 18, 440–447.

Róg, T., Vattulainen, I., Jansen, M., Ikonen, I., Karttunen, M., 2008. Comparison of cholesterol and its direct precursors along the biosynthetic pathway: effects of cholesterol, desmosterol, and 7-dehydrocholesterol on saturated and unsaturated lipids. J. Chem. Phys. 129, 154508.

Samuli, O.O.H., Róg, T., Karttunen, M., Vattulainen, I., 2007. Role of sterol type on lateral pressure profiles of lipid membranes affecting membrane protein functionality: comparison between cholesterol, desmosterol, 7-dehydrocholesterol, and ketosterol. J. Struct. Biol. 159, 311–323.

Sevcsik, E., Schütz, G.J., 2015. With or without rafts? Alternative views on cell membranes. Bioessays 38, 129–139.

Sezgin, E., Levental, I., Grzybek, M., Schwarzmann, G., Mueller, V., Honigmann, A., Belov, V.N., Eggeling, C., Coskun, U., Simons, K., Schwille, P., 2012. Partitioning, diffusion, and ligand binding of raft lipid analogs in model and cellular plasma membranes. Biochim. Biophys. Acta 1818, 1777–1784.

Shaghaghi, M., Chen, M.-T., Hsueh, Y.-W., Zuckermann, M.J., Thewalt, J.L., 2016. Effect of sterol structure on the physical properties of 1-palmitoyl-2-oleoyl-sn-glycero-3-phosphocholine membranes determined using ^{2}H nuclear magnetic resonance. Langmuir 32, 7654–7663.

Shahedi, V., Orädd, G., Lindblom, G., 2006. Domain-formation in DOPC/SM bilayers studied by Pfg-NMR: effect of sterol structure. Biophys. J. 91, 2501–2507.

Simons, K., Sampaio, J.L., 2011. Membrane organization and lipid rafts. Cold Spring Harb. Perspect. Biol. 3, a004697.

Simonsen, A.C., Bagatolli, L.A., Duelund, L., Garvik, O., Ipsen, J.H., Mouritsen, O.G., 2009. Effects of seaweed sterols fucosterol and demosterol on lipid membranes. Biophys. J. 96 (606a) .

Simonsen, A.C., Bagatolli, L.A., 2004. Structure of spin-coated lipid films and domain formation in supported membranes formed by hydration. Langmuir 20, 9720–9728.

Tapiero, H., Townsend, D.M., Tew, K.D., 2002. Phytosterols in the prevention of human pathologies. Biomed. Pharmacother. 57, 321–325.

Vainio, S., Jansen, M., Koivusalo, M., Róg, T., Karttunen, M., Vattulainen, I., Ikonen, I., 2006. Significance of sterol structural specificity. Desmosterol cannot replace cholesterol in lipid rafts. J. Biol. Chem. 281, 348–355.

Vilchèze, C., McMullen, T.P., McElhaney, R.N., Bittman, R., 1996. The effect of side-chain analogues of cholesterol on the thermotropic phase behavior of 1-stearoyl-2-oleoylphosphatidylcholine bilayers: a differential scanning calorimetric study. Biochim. Biophys. Acta 1279, 235–242.

Vist, M.R., Davis, J.H., 1990. Phase equilibria of cholesterol/dipalmitoylphosphatidylcholine mixtures: deuterium nuclear magnetic resonance and differential scanning calorimetry. Biochemistry 29, 451–464.

Yi, J., Knudsen, T.A., Nielsen, A.-L., Duelund, L., Christensen, M., Hervella, P., Needham, D., Mouritsen, O.G., 2016. Inhibition of cholesterol transport in an intestine cell model by pine-derived phytosterols. Chem. Phys. Lipids 200, 62–73.